

Kinetic theory of decentralized learning for smart active matter

Gerhard Jung,¹ Misaki Ozawa,¹ and Eric Bertin¹

¹*Université Grenoble Alpes, CNRS, LIPhy, 38000 Grenoble, France*

(Dated: January 8, 2025)

Smart active matter describes agents which can process information according to their individual policy to solve predefined tasks. We introduce a theoretical framework to study a decentralized learning process in which agents can locally exchange their policy to optimize their reward and thus attain target macroscopic states. We use our formalism to derive explicit hydrodynamic equations for the policy dynamics. We apply the theory to two different microscopic models where policies correspond either to fixed parameters similar to evolutionary dynamics, or to state-dependent controllers known from the field of robotics. We find good agreement between theoretical predictions and agent-based simulations. By deriving fundamental control parameters and uncertainty relations, our work lays the foundations for a statistical physics analysis of decentralized learning.

Decentralized optimization processes have been intensively studied in interdisciplinary fields using methods inspired from statistical physics, including the study of evolutionary and population dynamics in biology [1–4] and the investigation of social processes [5], such as opinion dynamics [6]. In addition, decentralized adaptation raises a growing interest in robotics and engineering [7–11], in particular to find more stable policies than typical centralized protocols [9, 10]. Robustness and flexibility may be enhanced by drawing inspiration from collective animal behavior [12]. Although standard experiments on robotic swarms are in practice often limited to less than a hundred robots, numerical simulations may account for much larger swarms, calling for a statistical physics approach to describe assemblies of small robots interacting through information exchange [10].

The idea of experimentally realizing large swarms of microrobots [13–15] as a way to build responsive or programmable metamaterials [16–19] is also at the core of the emerging field of smart active matter [20–24]. Along this soft robotics perspective, one tries to build large numbers of extremely simplified microrobots [25–28], whose size ranges from the granular scale [29, 30] down to the colloidal one [19, 31], and whose main features result from the physical properties of the soft material they are made of [32–35]. These soft microrobots may integrate simple computation capabilities [36], or may be controlled by an external computer through machine learning using, e.g., reinforcement learning techniques [37–46]. Although their starting points differ, both hard and soft robotics aim at building large assemblies of autonomous microrobots with communication and computation capabilities leading to adaptative collective behaviors [10, 11, 22, 23, 26, 47, 48]. This goal is also shared by the emerging topic of biological metamaterials, consisting for instance of insects aggregates [49, 50].

The ongoing experimental and numerical development of smart active matter calls for appropriate theoretical approaches to describe its collective properties. Early contributions in this direction include models of individual [51–55] or collective navigation of active parti-

cles [56, 57], or of pedestrians in a dense crowd [58, 59]. Stochastic thermodynamic may also be relevant to describe smart active matter [60, 61]. Yet, apart from some first steps [60], a theoretical framework to describe the collective behavior of adaptive agents exchanging information with their neighbors, as found in experiments with small robots [7–11], is still lacking.

In this Letter, we develop a statistical physics framework based on kinetic theory to describe decentralized learning in smart active matter with local information exchange. In contrast to usual active matter [62–64], smart active matter is made of agents having the ability to communicate, to respond to external stimuli and to adapt their behavior to attain targeted collective properties. The behavior of individual agents is determined by a ‘policy’, i.e., a set of rules controlling their dynamics, whose parameters can be tuned. Among the modeling approaches used to characterize active matter, kinetic theories have played an important role by providing a framework to derive macroscopic hydrodynamic equations from microscopic collision rules [65–69]. Here, we describe decentralized learning via the exchange of policies between neighboring agents, akin to collision rules. Such binary exchange rules set the stage for a kinetic theory framework, within which we systematically derive macroscopic hydrodynamic equations for the time-evolution of policies starting from agent-based models.

Agent-based model of decentralized learning – We consider a generic system of N agents in d dimensions representing, e.g., small robots [10]. Agents are located at position \mathbf{x} , move at velocity \mathbf{v} with an overdamped dynamics, and diffuse with a positional diffusion coefficient D_0 . Agents sense their environment (e.g., external fields or properties of neighboring particles) to control their dynamical rules. The set of adjustable parameters controlling the dynamics, which are specific to each agent, is here generically called the agent’s policy \mathcal{P} . In the examples below, the policy either corresponds to the agent’s angular diffusion coefficient, or to the response of the self-propulsion speed to an external stimulus. The state \mathcal{S} of an agent gathers internal physical variables (e.g., orien-

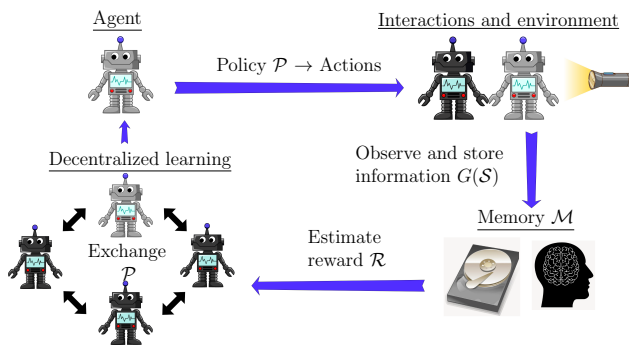


FIG. 1. Sketch of the decentralized learning procedure described in the manuscript.

tation, self-propulsion velocity, etc.) and sensors outputs such as measured light intensity. Agents can then process observed states and extract the signal $G(\mathcal{S})$, which fluctuates with a characteristic frequency τ_G^{-1} . The signal can be stored in the ‘memory’ \mathcal{M} via the running average $\mathcal{M}(t)$ through

$$\frac{d\mathcal{M}}{dt} = -\frac{1}{\tau_{\mathcal{M}}} (\mathcal{M} - G(\mathcal{S})), \quad (1)$$

on the memory time scale $\tau_{\mathcal{M}}$. All quantities \mathcal{S} , \mathcal{M} , and \mathcal{P} may be multi-component vectors. To lighten the presentation of the general formalism, we mostly stick to the scalar case, but the multi-component vector formalism is presented in the supplemental material (SM) [70].

To enable learning, agents can exchange information about the efficiency of their individual policies to reach a targeted collective behavior. This efficiency is quantified by a reward function $\mathcal{R}(\mathcal{M})$, which rewards agents following the targeted collective behavior. Comparing its own reward with other agents enables each agent to learn improved policies (see Fig. 1 for an illustration). The overall goal of each agent is to learn and optimize a policy \mathcal{P} maximizing the reward function. Agents are therefore randomly selected with a rate $\lambda_E = \tau_E^{-1}$, called the exchange rate (τ_E is the exchange time). Once selected, an agent i iterates over all neighbors n , chosen in random order within the interactions radius r_c . For each selected neighbor n , agent i becomes a teacher (and agent n the student) with a probability $p_T(\mathcal{R}_i, \mathcal{R}_n)$ given by

$$p_T(\mathcal{R}_i, \mathcal{R}_n) = \frac{1}{2} (1 + \tanh[\alpha_T(\mathcal{R}_i - \mathcal{R}_n)]), \quad (2)$$

where $\mathcal{R}_i = \mathcal{R}(\mathcal{M}_i)$ and $\mathcal{R}_n = \mathcal{R}(\mathcal{M}_n)$, and α_T is a parameter. Otherwise, agent n is the teacher and agent i is the student. In either case, the student updates its policy \mathcal{P}_S and memory \mathcal{M}_S by taking the corresponding values of the teacher, $\mathcal{P}_S := \mathcal{P}_T$ and $\mathcal{M}_S := \mathcal{M}_T$. The memory of the student is updated together with the policy to make its reward consistent with the updated policy [10]. The parameter α_T in Eq. (2) controls the sharpness of p_T , and may be interpreted as the precision

with which agents evaluate and communicate the reward \mathcal{R} . To enhance adaptability, we also include a small rate of spontaneous policy changes. By analogy with evolutionary processes in biology, we call these spontaneous changes ‘mutations’ [71] and model them as a diffusion process in policy space with diffusion coefficient D_M .

Kinetic theory of decentralized learning – To obtain a statistical description of the above agent-based model and derive the time-evolution for the statistics of policies \mathcal{P} , we introduce a kinetic theory framework. Learning events between two agents are treated by analogy with binary collisions in usual kinetic theory. In this framework, an assembly of a large number N of agents is described by a single-agent phase-space density $f(\mathcal{S}, \mathcal{M}, \mathcal{P}, \mathbf{x}, t)$ characterizing the probability to find an agent at time t at position \mathbf{x} , in state \mathcal{S} , with memory \mathcal{M} and policy \mathcal{P} . The time-evolution of $f(\mathcal{S}, \mathcal{M}, \mathcal{P}, \mathbf{x}, t)$ formally reads

$$\frac{\partial f}{\partial t} = \mathcal{I}_{\text{phys}}[f] + \mathcal{I}_{\text{sens}}[f] + \mathcal{I}_{\text{mem}}[f] + \mathcal{I}_{\text{pol}}[f]. \quad (3)$$

The term $\mathcal{I}_{\text{phys}}[f]$ describes the physical part of agents dynamics, e.g., their motion, angular dynamics and possibly physical interactions, and $\mathcal{I}_{\text{sens}}[f]$ defines the dynamics of the sensor output. The term $\mathcal{I}_{\text{mem}}[f]$ in Eq. (3) encodes the memory dynamics given in Eq. (1). Finally, the term $\mathcal{I}_{\text{pol}}[f]$ accounts for the dynamics of the policy \mathcal{P} , which includes diffusive mutations and communication-driven decentralized learning,

$$\mathcal{I}_{\text{pol}}[f] = D_M \frac{\partial^2 f}{\partial \mathcal{P}^2} + \mathcal{I}_{\text{learn}}[f]. \quad (4)$$

The learning term $\mathcal{I}_{\text{learn}}[f]$ represents the exchange of information between neighboring agents regarding their policies and the corresponding rewards. Mathematically, the term $\mathcal{I}_{\text{learn}}[f]$ is a bilinear integral term accounting for collision-like, binary learning events. The explicit, but lengthy, expression of $\mathcal{I}_{\text{learn}}[f]$ is reported in the End Matter (EM) section. We assume in this manuscript a time scale separation $\tau_G \ll \tau_{\mathcal{M}} \ll \tau_E$, i.e., a hierarchy of time scales separating signal dynamics τ_G , memory $\tau_{\mathcal{M}}$ and exchange rate τ_E . As a result, information advection by particle motion dominates over information propagation due to the finite communication range between agents. Within this approximation, our theory is thus purely local, however, it can be generalized to take into account the non-locality of communications or overlapping time scales.

To characterize the policy statistics, we assume that the reduced phase-space density

$$\varphi_0(\mathcal{P}, \mathbf{x}, t) = \int d\mathcal{S} \int d\mathcal{M} f(\mathcal{S}, \mathcal{M}, \mathcal{P}, \mathbf{x}, t) \quad (5)$$

is approximately Gaussian and can be described by its lowest-order moments. We also define the policy-dependent average memory,

$$\mu_{\mathcal{M}}(\mathcal{P}, \mathbf{x}, t) = \varphi_0^{-1} \int d\mathcal{S} \int d\mathcal{M} \mathcal{M} f(\mathcal{S}, \mathcal{M}, \mathcal{P}, \mathbf{x}, t). \quad (6)$$

The reduction steps from $f(\mathcal{S}, \mathcal{M}, \mathcal{P})$ to $\varphi_0(\mathcal{P})$ and

$\mu_{\mathcal{M}}(\mathcal{P})$ are described in the EM section. To keep the problem tractable, we expand $\mu_{\mathcal{M}}(\mathcal{P}, \mathbf{x}, t)$ around a pre-defined policy value \mathcal{P}_E , which should be a rough estimate of the optimal policy, yielding (dropping \mathbf{x} and t)

$$\mu_{\mathcal{M}}(\mathcal{P}) = \mu_{\mathcal{M}}^{(0)} + \mu_{\mathcal{M}}^{(1)}(\mathcal{P} - \mathcal{P}_E) + \dots \quad (7)$$

The quantities $\mu_{\mathcal{M}}^{(n)}$ are model-specific, and can be determined explicitly under the time scale separation hypothesis [70]. We further introduce the agent density $\rho(\mathbf{x}, t) = \int d\mathcal{P} \varphi_0(\mathcal{P}, \mathbf{x}, t)$, the average policy $\mu(\mathbf{x}, t)$ and its variance, called diversity, $\sigma^2(\mathbf{x}, t)$, defined as

$$\mu(\mathbf{x}, t) = \rho^{-1} \int d\mathcal{P} \mathcal{P} \varphi_0(\mathcal{P}, \mathbf{x}, t), \quad (8)$$

$$\sigma^2(\mathbf{x}, t) = \rho^{-1} \int d\mathcal{P} (\mathcal{P} - \mu(\mathbf{x}, t))^2 \varphi_0(\mathcal{P}, \mathbf{x}, t). \quad (9)$$

For spatially uniform fields $\rho(t)$, $\mu(t)$ and $\sigma^2(t)$, the evolution equations take the form,

$$\frac{d\mu}{dt} = \rho \sigma^2 F_1(\mu, \sigma^2; \mu_{\mathcal{M}}^{(n)}), \quad (10)$$

$$\frac{d\sigma^2}{dt} = 2D_M - \rho \sigma^4 F_2(\mu, \sigma^2; \mu_{\mathcal{M}}^{(n)}), \quad (11)$$

where $F_m(\mu, \sigma^2; \mu_{\mathcal{M}}^{(n)})$ are model-specific polynomials [70] depending on the parameters $\mu_{\mathcal{M}}^{(n)}(t)$ introduced in Eq. (7), which can be determined independently. The closed equations (10), (11) for the policy dynamics are one of the major results of this work. The full hydrodynamic equations including space-dependent fields are derived for two specific models in the SM [70]. Importantly, we can already draw some non-trivial general conclusions from Eqs. (10) and (11): (i) The derivative $\dot{\mu}(t)$ is proportional to the density $\rho(t)$ highlighting the many-body character of policy dynamics. Similarly, it is proportional to the diversity $\sigma^2(t)$, thus vanishing density or diversity imply vanishing adaptation rate $\dot{\mu}(t)$, consistent with Fisher's fundamental theorem of natural selection [72]. (ii) On time scales $t > \tau_{\mathcal{M}}$ with convex fitness function, we have $F_2(\mu(t), \sigma^2(t); \mu_{\mathcal{M}}^{(n)}(t)) > 0$ and thus $\sigma^2(t)$ decays monotonically in the absence of mutations. (iii) This emphasizes the importance of mutations D_M to maintain a sufficient level of diversity and thus enable efficient optimization. Qualitatively, mutations therefore play a role similar to driving in athermal physical systems, as they break detailed balance and maintain a steady-state dynamics at large time.

Phototactic, diffusive agents – As a first application of the above framework, we study a model of phototactic microswimmers ($d = 2$) with decentralized learning capabilities. Each swimmer moves at speed v_0 in a direction given by its orientation angle θ in the (x, y) -plane, which defines the state $\mathcal{S} = \theta$. As for active Brownian particles [73], orientation can change randomly via rotational diffusion with strength D_θ , but also via tumbling events towards the x -direction (direction of the light source) [74]. Physical interactions between microswim-

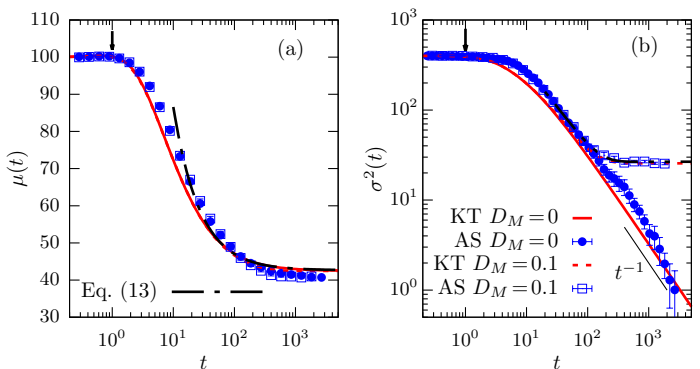


FIG. 2. Adaptation of the microswimmer model to a constant target velocity $V_T = 0.85$: Results of kinetic theory (KT) and agent-based simulations (AS) without mutations ($D_M = 0$) and with mutations ($D_M = 0.1$). The vertical arrow indicates $\tau_{\mathcal{M}} = 1$. (a) Average policy (rotation diffusion) $\mu(t)$; (b) diversity $\sigma^2(t)$. The black dashed-dotted curve is Eq. (12) fitted to the AS data with $D_M = 0.1$.

mers are neglected. The target state is a macroscopic flow along the x -axis in which the ensemble-averaged velocity $\bar{V}_x(D_\theta) = \langle V_x \rangle_{D_\theta}$ is equal to $V_T < v_0$. This target state is achieved via a decentralized learning procedure in which each agent measures its velocity $G(\mathcal{S}) = V_x = v_0 \cos \theta$ and adapts its rotational diffusion coefficient $\mathcal{P} = D_\theta$ (i.e., its policy) by maximizing the reward function, $\mathcal{R}(\mathcal{M}) = 1 - (\mathcal{M} - V_T)^2$. Importantly, although physical interactions are neglected, learning leads to collective effects. The asymptotic solutions of Eqs. (10) and (11) (detailed derivations in [70]) read,

$$\sigma^2(t) = \sqrt{\frac{2D_M}{\lambda_0}} \frac{1}{\tanh(\sqrt{2D_M \lambda_0}(\tau_0 + t))} \quad (12)$$

$$\mu(t) = D_{\theta, T} - \frac{\mu_0 \sqrt{2D_M \lambda_0}}{\sinh(\sqrt{2D_M \lambda_0}(\tau_0 + t))}, \quad (13)$$

which boil down to $\sigma^2(t) = [\lambda_0(\tau_0 + t)]^{-1}$ and $\mu(t) = D_{\theta, T} - \mu_0/(\tau_0 + t)$ for $D_M \rightarrow 0$. The parameter $\lambda_0 = 4\lambda_E \alpha_T \rho V_E'^2$ is a characteristic rate, where $V_E' = \partial \bar{V}_x(D_\theta) / \partial D_\theta |_{D_\theta = D_{\theta, E}}$ is the response of the average state to policy changes. The parameters τ_0 and μ_0 depend on initial conditions, and $D_{\theta, E} = \mathcal{P}_E$ is the pre-defined policy used in Eq. (7). When $D_M \geq 0$, $\sigma^2(t)$ converges to a plateau value $\sigma_\infty^2 = \sqrt{2D_M}/\lambda_0$ when $t \rightarrow \infty$, while $\mu(t)$ converges to the optimal policy $D_{\theta, T}$. The convergence of both $\sigma^2(t)$ and $\mu(t)$ occurs over the learning time $\tau_L = (2D_M \lambda_0)^{-1/2}$. Importantly, our theoretical analysis reveals two important control parameters: the rate λ_0 and the mutation strength D_M . The effect of the mutation rate D_M is characterized by the ‘uncertainty relation’ $\tau_L \sigma_\infty^2 = \lambda_0^{-1}$, where both τ_L and σ_∞^2 depend on D_M , while λ_0 is independent of D_M . The uncertainty relation states that quick convergence and adaptability (i.e., a small τ_L) obtained by increasing the mutation

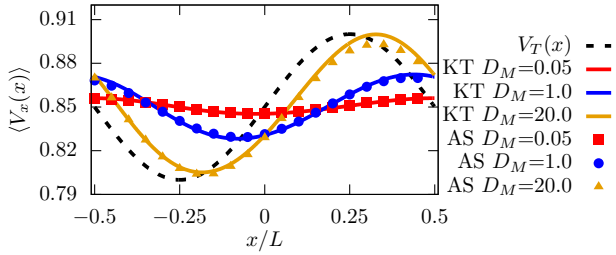


FIG. 3. Adaptation of the microswimmer model to a space-dependent target $V_T(x) = 0.85 + 0.05 \sin(2\pi x/L)$ (black-dashed line). Results obtained by kinetic theory (KT) and agent-based simulations (AS) are shown for different mutation rates D_M .

rate D_M comes at the cost of having large fluctuations around the target policy (i.e., a large σ_∞^2), in turn implying collective fluctuations around the target state, since $\text{Var}(N^{-1} \sum_{i=1}^N V_{x,i}) \propto \sigma_\infty^2/N$. Predictions of the kinetic theory are successfully compared to agent-based simulations in Fig. 2. Equation (12) can be used to fit the long-time behavior of $\sigma^2(t)$ on agent-based simulations data (see Fig. 2) to determine λ_0 and D_M , as on experimental data where such parameters are unknown. We get $D_M^{\text{fit}} = 0.094 \pm 0.002$ and $\lambda_0^{\text{fit}} = (2.65 \pm 0.01) \cdot 10^{-4}$, which compare well to the agent-based model values $D_M = 0.1$ and $\lambda_0 = 2.655 \cdot 10^{-4}$.

We now consider a space-dependent target velocity $V_T(x) = V_T^s + V_T^\Delta \sin(2\pi x/L)$ in a system of size L with periodic boundary conditions. The reward function thus also becomes space-dependent, $\mathcal{R}(\mathcal{M}, x) = 1 - (\mathcal{M} - V_T(x))^2$. At leading order, the steady-state average policy $\mu(x)$ satisfies [70],

$$-V_T^s \nabla \mu(x) - \sqrt{2D_M \lambda_L} (\mu(x) - D_{\theta,T}(x)) = 0, \quad (14)$$

where $D_{\theta,T}(x)$ is the optimal policy maximizing the local reward. We find for the average local velocity

$$\langle V_x(x) \rangle = V_T^s + V_x^\Delta(\phi) \sin(2\pi x/L - \phi), \quad (15)$$

with a phase ϕ given by $\tan(\phi) = 2\pi V_T^s / (\sqrt{2D_M \lambda_0} L)$ and an amplitude $V_x^\Delta(\phi) = V_T^\Delta \cos(\phi)$. Agents with small mutation rates travel across the system faster than they can adapt to the local target $V_T(x)$, therefore adopting an average speed V_T^s . In Fig. 3, we compare this predicted behavior by kinetic theory to agent-based simulations and find very good agreement for both the mutation-rate dependent amplitude $V_x^\Delta(D_M)$ and the phase $\phi(D_M)$. Our results emphasize the importance of the mutation rate D_M to maintain diversity and therefore being able to continuously adapt to space- and time-dependent targets.

Light-sensing robots – We also study a model featuring robots ($d = 1$) which attempt to maximize light collected from a heterogeneous light field $I(x)$. The state of a robot is $\mathcal{S} = (I, v)$, where I is the local light intensity measured by a sensor, and v is the robot velocity

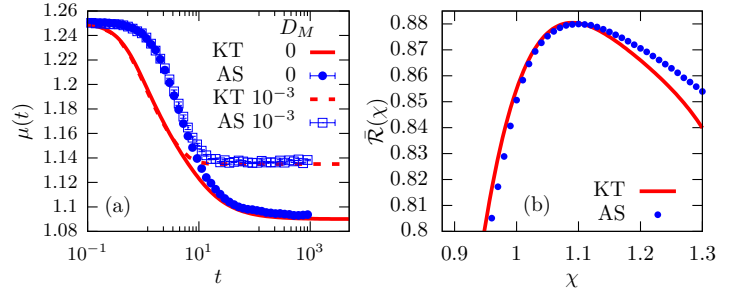


FIG. 4. Adaptation of the light-sensing robot model to maximize collected light: Kinetic theory (KT) and agent-based simulations (AS) without mutations ($D_M = 0$) and with mutations ($D_M = 10^{-3}$). (a) Average policy $\mu(t) = \langle \chi \rangle$; (b) Average reward $\bar{\mathcal{R}}(\chi)$ for robots with a given policy χ .

(diffusion is neglected, $D_0 = 0$). The memory \mathcal{M} averages the measured light intensity according to Eq. (1), with $G(\mathcal{S}) = I$. A state-dependent controller adapts the robot's speed $v(I) = v_0 - \chi I$, keeping $v(I) > v_{\min}$. The parameter χ thus defines the sensitivity with which the robot reacts to the external light. Robots adapt the policy $\mathcal{P} = \chi$ to maximize the collected light, using a reward $\mathcal{R}(\mathcal{M}) = \mathcal{M}$. Figure 4(a) shows that kinetic theory successfully describes the optimization of the controller (theoretical calculations in SM [70]), by predicting the long-time behavior of $\mu(t)$. In the absence of mutations ($D_M = 0$), the diversity $\sigma^2(t)$ goes to zero and $\mu(t)$ approaches the maximal reward around $\chi_T = 1.09$ [see Fig. 4(b)]. However, for $D_M > 0$, mutations cause the robots to learn a distribution of policies with $\sigma_\infty^2 > 0$. Importantly, the underlying model implies a pronounced asymmetry $\bar{\mathcal{R}}(\chi_T + \epsilon) > \bar{\mathcal{R}}(\chi_T - \epsilon)$, $\epsilon > 0$ [Fig. 4(b)], where $\bar{\mathcal{R}}(\chi) = \mathcal{R}(\mu_{\mathcal{M}}(\chi))$ is the average steady-state reward for an agent with policy χ . This makes it preferable to adapt for $t \rightarrow \infty$ to $\mu_\infty > \chi_T$ in the presence of mutations, as observed in the agent-based simulations. Expanding $\mu_{\mathcal{M}}$ to fourth order in Eq. (7), our kinetic theory provides a quantitative prediction of μ_∞ [Fig. 4(a)].

Conclusion and outlook – We proposed a kinetic theory framework for decentralized learning in smart active matter, in which agents maximize their reward \mathcal{R} by learning improved policies \mathcal{P} from neighboring agents, to reach a target collective state. This approach enables the derivation of space-dependent field equations describing the time-dependence of policy distributions. This framework has been applied to two explicit models, and predictions favorably compared to numerical simulations of the agent-based model, already showing a rich phenomenology. Future research direction may include the analysis of learning with different interaction ranges, multi-dimensional policies and more complex reward functions. While we considered for simplicity a limit of separated time scales between physical, memory and learning dynamics, our framework allows for systematic improve-

ments over this approximation, notably taking into account the effect of the communication range. In addition, it would also be of interest to investigate the generality of the uncertainty relation linking learning time and policy fluctuations.

Acknowledgments – The authors are grateful to Olivier Dauchot for stimulating discussions. This work has been supported by MIAI@Grenoble Alpes, (ANR-19-P3IA-0003).

-
- [1] B. Drossel, Biological evolution and statistical physics, *Advances in physics* **50**, 209 (2001).
- [2] G. Sella and A. E. Hirsh, The application of statistical physics to evolutionary biology, *Proceedings of the National Academy of Sciences* **102**, 9541 (2005).
- [3] B. Houchmandzadeh and M. Vallade, The fixation probability of a beneficial mutation in a geographically structured population, *New Journal of Physics* **13**, 073020 (2011).
- [4] N. Chia and N. Goldenfeld, Statistical mechanics of horizontal gene transfer in evolutionary ecology, *Journal of Statistical Physics* **142**, 1287 (2011).
- [5] C. Castellano, S. Fortunato, and V. Loreto, Statistical physics of social dynamics, *Rev. Mod. Phys.* **81**, 591 (2009).
- [6] J. Lorenz, Continuous opinion dynamics under bounded confidence: A survey, *International Journal of Modern Physics C* **18**, 1819 (2007).
- [7] R. A. Watson, S. G. Ficici, and J. B. Pollack, Embodied evolution: Distributing an evolutionary algorithm in a population of robots, *Robotics and Autonomous Systems* **39**, 1 (2002).
- [8] N. Bredeche, E. Haasdijk, and A. Prieto, Embodied evolution in collective robotics: A review, *Frontiers in Robotics and AI* **5**, 10.3389/frobt.2018.00012 (2018).
- [9] P. Long, T. Fan, X. Liao, W. Liu, H. Zhang, and J. Pan, Towards optimally decentralized multi-robot collision avoidance via deep reinforcement learning, in *2018 IEEE international conference on robotics and automation (ICRA)* (IEEE, 2018) pp. 6252–6259.
- [10] M. Y. Ben Zion, J. Fersula, N. Bredeche, and O. Dauchot, Morphological computation and decentralized learning in a swarm of sterically interacting robots, *Science Robotics* **8**, eabo6140 (2023).
- [11] N. Bredeche and N. Fontbonne, Social learning in swarm robotics, *Philosophical Transactions of the Royal Society B: Biological Sciences* **377**, 20200309 (2022).
- [12] M. Verdoucq, G. Theraulaz, R. Escobedo, C. Sire, and G. Hattenberger, Bio-inspired control for collective motion in swarms of drones, in *2022 International Conference on Unmanned Aircraft Systems (ICUAS)* (2022) pp. 1626–1631.
- [13] J. Wang, G. Wang, H. Chen, Y. Liu, P. Wang, D. Yuan, X. Ma, X. Xu, Z. Cheng, B. Ji, M. Yang, J. Shuai, F. Ye, J. Wang, Y. Jiao, and L. Liu, Robo-matter towards reconfigurable multifunctional smart materials, *Nat. Commun.* **15**, 8853 (2024).
- [14] D. Ma, J. Chen, S. Cutler, and K. Petersen, Smarticle 2.0: Design of scalable, entangled smart matter, in *Distributed Autonomous Robotic Systems*, edited by J. Bourgeois, J. Paik, B. Piranda, J. Werfel, S. Hauert, A. Pieron, H. Hamann, T. L. Lam, F. Matsuno, N. Mehr, and A. Makhoul (Springer Nature Switzerland, Cham, 2024) pp. 509–522.
- [15] Y. Ozkan-Aydin, D. I. Goldman, and M. S. Bhamla, Collective dynamics in entangled worm and robot blobs, *Proc. Natl. Acad. Sci. USA* **118**, e2010542118 (2021).
- [16] S. Li, B. Dutta, S. Cannon, J. J. Daymude, R. Avinery, E. Aydin, A. W. Richa, D. I. Goldman, and D. Randall, Programming active cohesive granular matter with mechanically induced phase changes, *Science Advances* **7**, eabe8494 (2021).
- [17] Y. Zhou, J. Zu, and J. Liu, Programmable intelligent liquid matter: material, science and technology, *Journal of Micromechanics and Microengineering* **32**, 103001 (2022).
- [18] A. Kotikian, C. McMahan, E. C. Davidson, J. M. Muhammad, R. D. Weeks, C. Daraio, and J. A. Lewis, Untethered soft robotic matter with passive control of shape morphing and propulsion, *Science Robotics* **4**, eaax7044 (2019).
- [19] Z. Zeravcic, V. N. Manoharan, and M. P. Brenner, Colloquium: Toward living matter with colloidal particles, *Rev. Mod. Phys.* **89**, 031001 (2017).
- [20] M. Pishvar and R. L. Harne, Foundations for soft, smart matter by active mechanical metamaterials, *Advanced Science* **7**, 2001384 (2020).
- [21] F. Cichos, K. Gustavsson, B. Mehlig, and G. Volpe, Machine learning for active matter, *Nat. Mach. Intell.* **2**, 94–103 (2020).
- [22] C. Kaspar, B. J. Ravoo, W. G. van der Wiel, S. V. Wegner, and W. H. P. Pernice, The rise of intelligent matter, *Nature* **594**, 345 (2021).
- [23] H. Levine and D. I. Goldman, Physics of smart active matter: integrating active matter and control to gain insights into living systems, *Soft Matter* **19**, 4204 (2023).
- [24] D. I. Goldman and D. Z. Rocklin, Robot swarms meet soft matter physics, *Science Robotics* **9**, eadn6035 (2024).
- [25] G. M. Whitesides, Soft robotics, *Angewandte Chemie International Edition* **57**, 4258 (2018).
- [26] C. Majidi, Soft-matter engineering for soft robotics, *Advanced Materials Technologies* **4**, 1800477 (2019).
- [27] A. C. H. Tsang, E. Demir, Y. Ding, and O. S. Pak, Roads to smart artificial microswimmers, *Advanced Intelligent Systems* **2**, 1900137 (2020).
- [28] L. Xu, R. J. Wagner, S. Liu, Q. He, T. Li, W. Pan, Y. Feng, H. Feng, Q. Meng, X. Zou, Y. Fu, X. Shi, D. Zhao, J. Ding, and F. J. Vernerey, Locomotion of an untethered, worm-inspired soft robot driven by a shape-memory alloy skeleton, *Sci. Rep.* **12**, 12392 (2022).
- [29] B. Saintyves, M. Spenko, and H. M. Jaeger, A self-organizing robotic aggregate using solid and liquid-like collective states, *Science Robotics* **9**, eadh4130 (2024).
- [30] W. Savoie, T. A. Berrueta, Z. Jackson, A. Pervan, R. Warkentin, S. Li, T. D. Murphey, K. Wiesenfeld, and D. I. Goldman, A robot made of robots: Emergent transport and control of a smarticle ensemble, *Science Robotics* **4**, eaax4316 (2019).
- [31] A. T. Liu, M. Hempel, J. F. Yang, A. M. Brooks, A. Pervan, V. B. Koman, G. Zhang, D. Kozawa, S. Yang, D. I. Goldman, M. Z. Miskin, A. W. Richa, D. Randall, T. D. Murphey, T. Palacios, and M. S. Strano, Colloidal robotics, *Nat. Mater.* **22**, 1453–1462 (2023).

- [32] M. Stern, C. Arinze, L. Perez, and A. Murugan, Supervised learning through physical changes in a mechanical system, *Proc. Natl. Acad. Sci. USA* **117**, 14843 (2020).
- [33] M. Stern, M. B. Pinson, and A. Murugan, Continual learning of multiple memories in mechanical networks, *Phys. Rev. X* **10**, 031044 (2020).
- [34] S. Dillavou, M. Stern, A. J. Liu, and D. J. Durian, Demonstration of decentralized physics-driven learning, *Phys. Rev. Appl.* **18**, 014040 (2022).
- [35] R. Mandal, R. Huang, M. Fruchart, P. G. Moerman, S. Vaikuntanathan, A. Murugan, and V. Vitelli, [Learning dynamical behaviors in physical systems](#) (2024), arXiv:2406.07856 [cond-mat.soft].
- [36] M. Garrad, G. Soter, A. T. Conn, H. Hauser, and J. Rossiter, A soft matter computer for soft robots, *Science Robotics* **4**, eaaw6060 (2019).
- [37] R. Muinos-Landin, A. Fischer, V. Holubec, and F. Cichos, Reinforcement learning with artificial microswimmers, *Science Robotics* **6**, eabd9285 (2021).
- [38] F. Cichos, S. Muiños Landin, and R. Pradip, Chapter 5 - artificial intelligence (ai) enhanced nanomotors and active matter, in *Intelligent Nanotechnology*, Materials Today, edited by Y. Zheng and Z. Wu (Elsevier, 2023) pp. 113–144.
- [39] S. Colabrese, K. Gustavsson, A. Celani, and L. Biferale, Flow navigation by smart microswimmers via reinforcement learning, *Phys. Rev. Lett.* **118**, 158004 (2017).
- [40] K. Gustavsson, L. Biferale, A. Celani, and S. Colabrese, Finding efficient swimming strategies in a three-dimensional chaotic flow by reinforcement learning, *The European Physical Journal E* **40**, 1 (2017).
- [41] M. Durve, F. Peruani, and A. Celani, Learning to flock through reinforcement, *Phys. Rev. E* **102**, 012601 (2020).
- [42] M. J. Falk, V. Alizadehyazdi, H. Jaeger, and A. Murugan, Learning to control active matter, *Phys. Rev. Res.* **3**, 033291 (2021).
- [43] K. Sankawong, J. J. Molina, M. S. Turner, and R. Yamamoto, Learning to swim efficiently in a nonuniform flow field, *Phys. Rev. E* **107**, 065102 (2023).
- [44] Z. Zou, Y. Liu, A. C. H. Tsang, Y.-N. Young, and O. S. Pak, Adaptive micro-locomotion in a dynamically changing environment via context detection, *Communications in Nonlinear Science and Numerical Simulation* **128**, 107666 (2024).
- [45] T. Xiong, Z. Liu, C. J. Ong, and L. Zhu, [Enabling micro-robotic chemotaxis via reset-free hierarchical reinforcement learning](#) (2024), arXiv:2408.07346 [cond-mat.soft].
- [46] J. Grauer, F. J. Schwarzendahl, H. Löwen, and B. Liebchen, Optimizing collective behavior of communicating active particles with machine learning, *Machine Learning: Science and Technology* **5**, 015014 (2024).
- [47] L. G. Mo C. and B. X., Challenges and attempts to make intelligent microswimmers, *Front. Phys.* **11**, 1279883 (2023).
- [48] L. Cazenille, M. Toquebiau, N. Lobato-Dauzier, A. Loi, L. Macabre, N. Aubert-Kato, A. Genot, and N. Bredeche, [Signaling and social learning in swarms of robots](#) (2024), arXiv:2411.11616 [cs.RO].
- [49] M. Tennenbaum, Z. Liu, D. Hu, and A. Fernandez-Nieves, Mechanics of fire ant aggregations, *Nat. Mater.* **15**, 54–59 (2016).
- [50] R. J. Wagner and F. J. Vernerey, Computational exploration of treadmilling and protrusion growth observed in fire ant rafts, *PLOS Computational Biology* **18**, 1 (2022).
- [51] B. Liebchen and H. Löwen, Optimal navigation strategies for active particles, *Europhysics Letters* **127**, 34003 (2019).
- [52] L. Piro, E. Tang, and R. Golestanian, Optimal navigation strategies for microswimmers on curved manifolds, *Phys. Rev. Res.* **3**, 023125 (2021).
- [53] L. Piro, B. Mahault, and R. Golestanian, Optimal navigation of microswimmers in complex and noisy environments, *New Journal of Physics* **24**, 093037 (2022).
- [54] L. Piro, R. Golestanian, and B. Mahault, Efficiency of navigation strategies for active particles in rugged landscapes, *Front. Phys.* **10**, 1034267 (2022).
- [55] M. Nasiri, H. Löwen, and B. Liebchen, Optimal active particle navigation meets machine learning, *Europhysics Letters* **142**, 17001 (2023).
- [56] F. Borra, M. Cencini, and A. Celani, Optimal collision avoidance in swarms of active brownian particles, *Journal of Statistical Mechanics: Theory and Experiment* **2021**, 083401 (2021).
- [57] L. Yang, J. Jiang, X. Gao, Q. Wang, Q. Dou, and L. Zhang, Autonomous environment-adaptive micro-robot swarm navigation enabled by deep learning-based real-time distribution planning, *Nature Machine Intelligence* **4**, 480 (2022).
- [58] I. Echeverría-Huarte and A. Nicolas, Body and mind: Decoding the dynamics of pedestrians and the effect of smartphone distraction by coupling mechanical and decisional processes, *Transportation Research Part C: Emerging Technologies* **157**, 104365 (2023).
- [59] T. Bonnemain, M. Butano, T. Bonnet, I. n. Echeverría-Huarte, A. Seguin, A. Nicolas, C. Appert-Rolland, and D. Ullmo, Pedestrians in static crowds are not grains, but game players, *Phys. Rev. E* **107**, 024612 (2023).
- [60] B. VanSaders and V. Vitelli, [Informational active matter](#), arXiv preprint arXiv:2302.07402 (2023).
- [61] L. Cocconi, B. Mahault, and L. Piro, [Dissipation-accuracy tradeoffs in autonomous control of smart active matter](#) (2024), arXiv:2409.12595 [cond-mat.stat-mech].
- [62] S. Ramaswamy, The mechanics and statistics of active matter, *Annual Review of Condensed Matter Physics* **1**, 323 (2010).
- [63] M. C. Marchetti, J. F. Joanny, S. Ramaswamy, T. B. Liverpool, J. Prost, M. Rao, and R. A. Simha, Hydrodynamics of soft active matter, *Rev. Mod. Phys.* **85**, 1143 (2013).
- [64] S. Ramaswamy, Active fluids, *Nat. Rev. Phys.* **1**, 640–642 (2019).
- [65] E. Bertin, M. Droz, and G. Grégoire, Boltzmann and hydrodynamic description for self-propelled particles, *Phys. Rev. E* **74**, 022101 (2006).
- [66] E. Bertin, M. Droz, and G. Grégoire, Hydrodynamic equations for self-propelled particles: microscopic derivation and stability analysis, *Journal of Physics A: Mathematical and Theoretical* **42**, 445001 (2009).
- [67] T. Ihle, Kinetic theory of flocking: Derivation of hydrodynamic equations, *Physical Review E—Statistical, Nonlinear, and Soft Matter Physics* **83**, 030901 (2011).
- [68] E. Bertin, H. Chaté, F. Ginelli, S. Mishra, A. Peshkov, and S. Ramaswamy, Mesoscopic theory for fluctuating active nematics, *New journal of physics* **15**, 085032 (2013).
- [69] T. Ihle, Towards a quantitative kinetic theory of polar active matter, *The European Physical Journal Special Topics* **223**, 1293 (2014).
- [70] See Supplemental Material at [URL will be inserted

by publisher] for technical details on the derivations of Eqs. (XX).

- [71] V. Chardès, A. Mazzolini, T. Mora, and A. M. Walczak, Evolutionary stability of antigenically escaping viruses, *Proceedings of the National Academy of Sciences* **120**, e2307712120 (2023), <https://www.pnas.org/doi/pdf/10.1073/pnas.2307712120>.
- [72] W. Ewens, An interpretation and proof of the fundamental theorem of natural selection, *Theoretical Population Biology* **36**, 167 (1989).
- [73] P. Romanczuk, M. Bär, W. Ebeling, B. Lindner, and L. Schimansky-Geier, Active brownian particles: From individual to collective stochastic dynamics, *The European Physical Journal Special Topics* **202**, 1 (2012).
- [74] M. Martin, A. Barzyk, E. Bertin, P. Peyla, and S. Rafai, Photofocusing: Light and flow of phototactic microswimmer suspension, *Phys. Rev. E* **93**, 051101 (2016).

End Matter – We describe here the general framework of kinetic theory of decentralized learning introduced in this work. Calculation details for specific models are reported in the SM [70].

The term $\mathcal{I}_{\text{learn}}[f]$, introduced in Eq. (4), can be formulated in a rather similar way as usual collision terms in kinetic theories. It is convenient to express $\mathcal{I}_{\text{learn}}[f]$ in a similar way as a master equation for a stochastic jump process, using a f -dependent effective transition rate $W_f(\mathcal{M}', \mathcal{P}'|\mathcal{M}, \mathcal{P}; \mathbf{x}, t)$ defined as,

$$\begin{aligned} W_f(\mathcal{M}', \mathcal{P}'|\mathcal{M}, \mathcal{P}; \mathbf{x}, t) &= 2\lambda_E \int d\mathcal{S}_2 \int d\mathcal{M}_2 \int d\mathcal{P}_2 \int d\mathbf{x}_2 K(\mathbf{x}_2, \mathbf{x}) \\ &\times p_T(\mathcal{R}(\mathcal{M}_2), \mathcal{R}(\mathcal{M})) f(\mathcal{S}_2, \mathcal{M}_2, \mathcal{P}_2, \mathbf{x}_2, t) \\ &\times \delta(\mathcal{P}' - \mathcal{P}_2) \delta(\mathcal{M}' - \mathcal{M}_2). \end{aligned} \quad (16)$$

The transition rate W_f encodes the microscopic learning dynamics of the agent model: the probability that a focus particle 1, at position \mathbf{x} and characterized by $(\mathcal{S}, \mathcal{M}, \mathcal{P})$, learns its memory $\mathcal{M}' = \mathcal{M}_2$ and policy $\mathcal{P}' = \mathcal{P}_2$ from a particle 2 at position \mathbf{x}_2 and with $(\mathcal{S}_2, \mathcal{M}_2, \mathcal{P}_2)$, is proportional to the communication rate λ_E , the distance-dependent kernel $K(\mathbf{x}_2, \mathbf{x})$, and to the teaching probability $p_T(\mathcal{R}(\mathcal{M}_2), \mathcal{R}(\mathcal{M}))$ (i.e., the probability that particle 2 becomes the teacher of particle 1), defined in Eq. (2). The kernel $K(\mathbf{x}_2, \mathbf{x})$ has a characteristic range δ_c , e.g., $K(\mathbf{x}_2, \mathbf{x}) = (2\pi\delta_c^2)^{-1} \exp[-(\mathbf{x}_2 - \mathbf{x})^2/2\delta_c^2]$ in 2D, and is normalized to 1. Note that if the agent learns the policy \mathcal{P}_2 it also adapts its memory to the value \mathcal{M}_2 in order to evaluate the correct reward associated with policy \mathcal{P}_2 . The state \mathcal{S} of particle 1 is not included in $W_f(\mathcal{M}', \mathcal{P}'|\mathcal{M}, \mathcal{P}; \mathbf{x}, t)$ because \mathcal{S} is not modified by the learning process. The factor of 2 in front of λ_E accounts for the fact that during one adaptation step either agent 1 is the teacher and agent 2 the student or the other way around.

Note also that at variance with usual kinetic theories (e.g., of gases, granular gases or active matter), the occurrence of learning interactions is not controlled by the kinetics of particle collisions, but rather by an imposed

communication rate λ_E , which in practice may be much smaller than the rate of particle encounter. We thus assume that information propagation due to the sole communication range, at a speed at most at the order of $\lambda_E\delta_c$, remains much slower than information advection by particle motion at a typical speed v_0 (i.e., we assume $\lambda_E\delta_c \ll v_0$). This means that we can neglect the distinction between \mathbf{x}_2 and \mathbf{x} in Eq. (16), thereby yielding a purely local expression of W_f ,

$$W_f(\mathcal{M}', \mathcal{P}'|\mathcal{M}, \mathcal{P}) = 2\lambda_E p_T(\mathcal{R}(\mathcal{M}'), \mathcal{R}(\mathcal{M})) f_0(\mathcal{M}', \mathcal{P}'), \quad (17)$$

where we have introduced the marginal distribution $f_0(\mathcal{M}, \mathcal{P}) = \int d\mathcal{S} f(\mathcal{S}, \mathcal{M}, \mathcal{P})$. Here, and in the following, we drop the explicit dependence on \mathbf{x} and t for the sake of brevity. The learning term $\mathcal{I}_{\text{learn}}[f]$ is formally obtained from an effective master equation, and takes the form,

$$\begin{aligned} \mathcal{I}_{\text{learn}}[f] &= \int d\mathcal{M}' \int d\mathcal{P}' [W_f(\mathcal{M}, \mathcal{P}|\mathcal{M}', \mathcal{P}') f(\mathcal{S}, \mathcal{M}', \mathcal{P}') \\ &\quad - W_f(\mathcal{M}', \mathcal{P}'|\mathcal{M}, \mathcal{P}) f(\mathcal{S}, \mathcal{M}, \mathcal{P})]. \end{aligned} \quad (18)$$

By inserting the explicit form of the transition rate in Eq. (17), the learning term can be written down explicitly,

$$\begin{aligned} \mathcal{I}_{\text{learn}}[f] &= \\ &2\lambda_E f_0(\mathcal{M}, \mathcal{P}) \int d\mathcal{M}' p_T(\mathcal{R}', \mathcal{R}) \int d\mathcal{P}' f(\mathcal{S}, \mathcal{M}', \mathcal{P}') \\ &\quad - 2\lambda_E f(\mathcal{S}, \mathcal{M}, \mathcal{P}) \int d\mathcal{M}' p_T(\mathcal{R}, \mathcal{R}') \int d\mathcal{P}' f_0(\mathcal{M}', \mathcal{P}'), \end{aligned} \quad (19)$$

with the shorthand notations $\mathcal{R} = \mathcal{R}(\mathcal{M})$ and $\mathcal{R}' = \mathcal{R}(\mathcal{M}')$. Writing decentralized learning in such a general way and thus introducing a framework for the systematic derivation of macroscopic hydrodynamic equations for population dynamics is one of the major results of this manuscript. In the following, we now aim at transforming these equations to derive macroscopic equations for the dynamics of policies.

In a first reduction step, we integrate out the dependence of f on the state \mathcal{S} and memory \mathcal{M} to focus on the macroscopic dynamics of policies. As a first approximation this can be achieved by assuming $\tau_G \ll \tau_{\mathcal{M}} \ll \tau_E$, i.e., that the time scale $\tau_{\mathcal{M}}$ is large enough to distinguish the fluctuations in the observations of $G(\mathcal{S})$ on a time scale τ_G from the relevant signal and that the learning occurs on time scales much larger than changes in the memory. When studying the time-dependence of f on a time scale $\tau_{\mathcal{M}}$, the physical interaction terms in $\mathcal{I}_{\text{phys}}[f]$ and the sensor dynamics $\mathcal{I}_{\text{sens}}[f]$ drop out. Using the explicit relation for the memory dynamics,

$$I_{\text{mem}}[f] = \tau_{\mathcal{M}}^{-1} \left(f(\mathcal{S}, \mathcal{M}, \mathcal{P}) + (\mathcal{M} - G(\mathcal{S})) \frac{\partial f(\mathcal{S}, \mathcal{M}, \mathcal{P})}{\partial \mathcal{M}} \right), \quad (20)$$

we find a closed equation for the time-dependence of the

marginal distribution,

$$\begin{aligned} \frac{\partial f_0(\mathcal{M}, \mathcal{P})}{\partial t} &= -\nabla J_0 + \tau_{\mathcal{M}}^{-1} \left(f_0 + (\mathcal{M} - \bar{G}(\mathcal{P})) \frac{\partial f_0}{\partial \mathcal{M}} \right) \\ &\quad + 2\lambda_E f_0 \int d\mathcal{M}' \tanh(\alpha_T(\mathcal{R} - \mathcal{R}')) \int d\mathcal{P}' f_0(\mathcal{M}', \mathcal{P}') \\ &\quad + D_M \frac{\partial^2}{\partial \mathcal{P}^2} f_0 \end{aligned} \quad (21)$$

with the current $J_0 = (\bar{V}(\mathcal{P}) - D_0 \nabla) f_0$. At this level, the details of the microscopic model thus only enter via the policy-dependent average of the observed information $\bar{G}(\mathcal{P}) := \langle G(\mathcal{S}) \rangle_{\mathcal{P}}$, and the policy-dependent average velocity $\bar{V}(\mathcal{P}) := \langle V \rangle_{\mathcal{P}}$. The brackets $\langle \dots \rangle_{\mathcal{P}}$ denote the policy-dependent ensemble average used as a proxy for the running average on a time scale $\tau_{\mathcal{M}}$ due to the assumed time scale separation.

As in the main text, we then introduce the marginal

phase-space distribution of policies [Eq. (5)], the agent density $\rho(\mathbf{x}, t) = \int d\mathcal{P} \varphi_0(\mathcal{P}, \mathbf{x}, t)$ and the average memory, $\mu_{\mathcal{M}}(\mathcal{P}, \mathbf{x}, t) = \varphi_0^{-1} \int d\mathcal{M} \mathcal{M} f_0(\mathcal{M}, \mathcal{P}, \mathbf{x}, t)$ [Eq. (6)]. To find closed equations we approximate the activation function to first order, $\tanh(\alpha_T(\mathcal{R} - \mathcal{R}')) = \alpha_T(\mathcal{R} - \mathcal{R}') + \mathcal{O}(\alpha_T^2(\mathcal{R} - \mathcal{R}'))$. After some calculations we find,

$$\begin{aligned} \frac{\partial \varphi_0(\mathcal{P})}{\partial t} &= -\nabla J + D_M \frac{\partial^2}{\partial \mathcal{P}^2} \varphi_0(\mathcal{P}) \\ &\quad - \tilde{\lambda}_E \rho \int d\mathcal{M} f_0(\mathcal{M}, \mathcal{P}) \mathcal{R}(\mathcal{M}) \\ &\quad + \tilde{\lambda}_E \varphi_0(\mathcal{P}) \int d\mathcal{P}' \int d\mathcal{M}' f_0(\mathcal{M}', \mathcal{P}') \mathcal{R}(\mathcal{M}'), \end{aligned} \quad (22)$$

with the policy current $J = (\bar{V}(\mathcal{P}) - D_0 \nabla) \varphi_0$. We also introduce the renormalized exchange rate, $\tilde{\lambda}_E = 2\lambda_E \alpha_T$. For the average memory we can derive,

$$\frac{\partial \mu_{\mathcal{M}}(\mathcal{P})}{\partial t} = \tau_{\mathcal{M}}^{-1} \left(\bar{G}(\mathcal{P}) - \mu_{\mathcal{M}}(\mathcal{P}) \right). \quad (23)$$

Supplemental Material for “Kinetic theory of decentralized learning for smart active matter”

Gerhard Jung, Misaki Ozawa, and Eric Bertin
(Dated: January 8, 2025)

In this supplemental material (SM) we provide details on the theoretical derivation of the kinetic theory. This includes theoretical details for the microswimmer model (Sec. I) and the light-sensing robot model (Sec. II), and the derivation of the multi-dimensional case (Sec. III).

I. DERIVATIONS FOR MODEL1: MICROSWIMMERS

The first model we analyze consists of non-interacting microswimmers in two-dimensions. Each swimmer is characterized by its individual rotational diffusion coefficient $D_\theta = \mathcal{P}$ which will also correspond to the policy we are aiming to optimize. Furthermore, the microswimmers tend to align into the direction of an external light source in the x -direction (see Fig. S1). In the model, the speed v_0 of the swimmer is constant, $\mathbf{v} = v_0 \mathbf{n}$ and thus only the heading vector $\mathbf{n} = (\cos \theta, \sin \theta)$ is fluctuating. Here, $\theta = \mathcal{S}$ is therefore the internal variable of interest. The interaction term then reads,

$$\mathcal{I}_{\text{phys}}[f] = \mathcal{I}_{\text{rot}}[f] + \mathcal{I}_{\text{bias}}[f], \quad (\text{S1})$$

$$\mathcal{I}_{\text{rot}}[f] = D_\theta \frac{\partial^2}{\partial \theta^2} f \quad (\text{S2})$$

$$\mathcal{I}_{\text{bias}}[f] = -\lambda_B f + \lambda_B P_B(\theta) f_0. \quad (\text{S3})$$

Here, λ_B is the rate with which the microswimmers tumble and bias their orientation θ towards the distribution $P_B(\theta)$, thus aligning with the x -axis. We assume that P_B is Gaussian with the standard deviation σ_B . In consequence, for a given bias strength, the microswimmer can adapt its average velocity $\langle V_x \rangle_{D_\theta}$ in x -direction by choosing a larger diffusion coefficient (small $\langle V_x \rangle$) or a smaller diffusion coefficient (large $\langle V_x \rangle$). This model is inspired by the behaviour of the microalga *Chlamydomonas Reinhardtii* which features negative phototaxis, a very similar model has already been analyzed theoretically [S1, S2].

A. Solving the microscopic physical model

Since the model is two-dimensional, to simplify calculations we introduce the complex vector notation, $n = n_x + i n_y = e^{i\theta}$. Therefore $n_x = \text{Re}(n)$ and $n_y = \text{Im}(n)$. To remove the dependence of the model on the orientation θ we expand

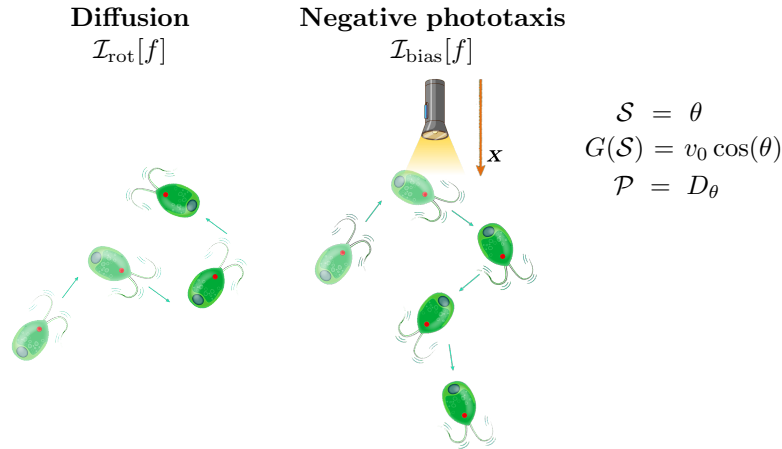


FIG. S1. Illustration of the two physical interaction terms. $\mathcal{I}_{\text{rot}}[f]$ just leads to random reorientation, while $\mathcal{I}_{\text{bias}}[f]$ describes (negative) phototaxis and thus biases the motion of the microswimmer towards the positive x -direction.

f using its Fourier-transform, $f_k = \int_{-\pi}^{\pi} d\theta e^{i\theta k} f(\theta)$. Following Refs. [S1, S3] we can thus derive the time-dependence of the distribution f_k without the contribution of memory and learning,

$$\frac{\partial f_k}{\partial t} + \frac{v_0}{2} (\nabla f_{k-1} + \nabla^* f_{k+1}) - D_0 \Delta f_k = -D_\theta k^2 f_k - \lambda_B (f_k - f_0 e^{-\sigma_B^2 k^2 / 2}). \quad (\text{S4})$$

For the memory term, $\mathcal{I}_{\text{mem}}[f]$ we choose $G(\mathcal{S}) = v_0 \cos \theta$, corresponding to the instantaneous velocity in x -direction. We thus find,

$$\int_{-\pi}^{\pi} d\theta \mathcal{I}_{\text{mem}}[f] = \tau_{\mathcal{M}}^{-1} \int_{-\pi}^{\pi} d\theta \left(f + (\mathcal{M} - v_0 \cos(\theta)) \frac{\partial f(\theta, \mathcal{M}, \mathcal{P}, \mathbf{x}, t)}{\partial \mathcal{M}} \right) \quad (\text{S5})$$

$$= \tau_{\mathcal{M}}^{-1} \left(f_0 + \left(\mathcal{M} \frac{\partial f_0}{\partial \mathcal{M}} - v_0 \frac{\partial \text{Re}(f_1)}{\partial \mathcal{M}} \right) \right) \quad (\text{S6})$$

$$\int_{-\pi}^{\pi} d\theta e^{i\theta} \mathcal{I}_{\text{mem}}[f] = \tau_{\mathcal{M}}^{-1} \left(f_1 + \left(\mathcal{M} \frac{\partial f_1}{\partial \mathcal{M}} - v_0 \frac{\partial \hat{f}_2}{\partial \mathcal{M}} \right) \right) \quad (\text{S7})$$

where we have defined $\hat{f}_2 = \int_{-\pi}^{\pi} d\theta e^{i\theta} \cos(\theta) f(\theta, \mathcal{M}, \mathcal{P}, \mathbf{x}, t) = \frac{1}{2}(f_0 + f_2)$. We are interested in the dynamics of the two lowest moments, the marginal distribution f_0 corresponding to the density and the first-order moment f_1 , which is related to the average velocity in x -direction, $\langle V_x \rangle = v_0 f_0^{-1} \text{Re}(f_1)$. For these two moments we find explicitly,

$$\begin{aligned} \frac{\partial f_0(\mathcal{M}, \mathcal{P}, \mathbf{x}, t)}{\partial t} &= -v_0 \text{Re}(\nabla^* f_1) + D_0 \Delta f_0 + \tau_{\mathcal{M}}^{-1} \left(f_0 + \left(\mathcal{M} \frac{\partial f_0}{\partial \mathcal{M}} - v_0 \frac{\partial f_1}{\partial \mathcal{M}} \right) \right) \\ &+ D_M \frac{\partial^2}{\partial \mathcal{P}^2} f_0 + 2\lambda_E f_0 \int d\mathcal{M}' \tanh(\alpha_T(\mathcal{R} - \mathcal{R}')) \int d\mathcal{P}' f'_0, \end{aligned} \quad (\text{S8})$$

$$\begin{aligned} \frac{\partial f_1(\mathcal{M}, \mathcal{P}, \mathbf{x}, t)}{\partial t} &= -\frac{v_0}{2} (\nabla f_0 + \nabla^* f_2) + D_0 \Delta f_1 - D_\theta f_1 - \lambda_B (f_1 - f_0 e^{-\sigma_B^2 / 2}) \\ &+ \tau_{\mathcal{M}}^{-1} \left(f_1 + \left(\mathcal{M} \frac{\partial f_1}{\partial \mathcal{M}} - \frac{v_0}{2} \left(\frac{\partial f_0}{\partial \mathcal{M}} + \frac{\partial f_2}{\partial \mathcal{M}} \right) \right) \right) + D_M \frac{\partial^2}{\partial \mathcal{P}^2} f_1 + \lambda_E f_0 \int d\mathcal{M}' \tanh(\alpha_T(\mathcal{R} - \mathcal{R}')) \int d\mathcal{P}' f'_1 \\ &- \lambda_E f_1 \int d\mathcal{M}' \tanh(\alpha_T(\mathcal{R} - \mathcal{R}')) \int d\mathcal{P}' f'_0, \end{aligned} \quad (\text{S9})$$

where $f'_k = f_k(\mathcal{M}', \mathcal{P}', \mathbf{x}, t)$. In the following, we will assume that the physical time scales λ_B^{-1} and D_θ^{-1} are much smaller than $\tau_{\mathcal{M}}$, λ_E^{-1} , D_M^{-1} , $\Delta L^2/D_0$ and $\Delta L/v_0$, where ΔL is a typical length scale in the system. Further, we will use $\partial f_1/\partial t$ to calculate $\partial \langle V_x(t) \rangle / \partial t$. This finally yields,

$$\frac{\partial \langle V_x(t) \rangle_{D_\theta}}{\partial t} = -D_\theta \langle V_x(t) \rangle_{D_\theta} - \lambda_B (\langle V_x(t) \rangle_{D_\theta} - v_0 e^{-\sigma_B^2 / 2}). \quad (\text{S10})$$

We can then solve the above equation analytically to find the steady state solution,

$$\bar{V}_x(D_\theta) = \langle V_x \rangle_{D_\theta} = v_0 \frac{\lambda_B e^{-\sigma_B^2 / 2}}{D_\theta + \lambda_B}. \quad (\text{S11})$$

By inserting this relation into the term, $v_0 \partial f_1 / \partial \mathcal{M} = \langle V_x \rangle_{D_\theta} \partial f_0 / \partial \mathcal{M}$ we find that $\bar{V}_x(D_\theta)$ directly corresponds to the term $\bar{G}(\mathcal{P})$ as introduced in Eq. (21) in the End Matter section of the main manuscript, i.e. the average of the information $G(\mathcal{S}) = V_x$ which is expected to be observed for an agent with policy \mathcal{P} . Importantly, one might also be able to find more complex analytical solutions, for example when there is no clear timescale separation between the physical timescales $\lambda_B^{-1} = \tau_G$ and the memory time scale $\tau_{\mathcal{M}}$. Additionally, when using a more complex physical model and $\mathcal{I}_{\text{phys}}[f]$ potentially features interactions between agents, one needs to make suitable approximations to find an analytical solution for $\bar{V}_x(D_\theta)$. This can be achieved by using standard approximations applied to kinetic theories [S3].

B. Hydrodynamic equations

As introduced in the main manuscript, we will choose as reward function, $\mathcal{R}(\mathcal{M}) = 1 - (\mathcal{M} - V_T)^2$. This enables us to expand f_0 in terms of its density, $\varphi_0(D_\theta, \mathbf{x}, t) = \int d\mathcal{M} f_0(\mathcal{M}, D_\theta, \mathbf{x}, t)$, the average memory, $\mu_{\mathcal{M}}(D_\theta, \mathbf{x}, t) = \varphi_0^{-1} \int d\mathcal{M} \mathcal{M} f_0(\mathcal{M}, D_\theta, \mathbf{x}, t)$ and the memory variance, $\sigma_{\mathcal{M}}^2(D_\theta, \mathbf{x}, t) = \varphi_0^{-1} \int d\mathcal{M} (\mathcal{M} - \mu_{\mathcal{M}}(D_\theta, \mathbf{x}, t))^2 f_0(\mathcal{M}, D_\theta, \mathbf{x}, t)$.

Finally, we can thus rewrite Eq. (22) in the main manuscript and find,

$$\begin{aligned} \frac{\partial \varphi_0(D_\theta, \mathbf{x}, t)}{\partial t} &= -\nabla \left(\bar{V}_x(D_\theta) + D_0 \nabla \right) \varphi_0 + \tilde{\lambda}_E \varphi_0 \int dD'_\theta \varphi_0(D'_\theta, \mathbf{x}, t) \left(\sigma_{\mathcal{M}}^2(D'_\theta, \mathbf{x}, t) + \mu_{\mathcal{M}}(D'_\theta, \mathbf{x}, t)^2 - 2V_T \mu_{\mathcal{M}}(D'_\theta, \mathbf{x}, t) \right) \\ &\quad + \tilde{\lambda}_E \varphi_0 \rho(\mathbf{x}, t) \left(2V_T \mu_{\mathcal{M}} - \mu_{\mathcal{M}}^2 - \sigma_{\mathcal{M}}^2 \right) + D_M \frac{\partial^2}{\partial D_\theta^2} \varphi_0 \end{aligned} \quad (\text{S12})$$

$$\begin{aligned} \frac{\partial \mu_{\mathcal{M}}(D_\theta, \mathbf{x}, t)}{\partial t} &= -\bar{V}_x(D_\theta) \nabla \mu_{\mathcal{M}} + D_0 \Delta \mu_{\mathcal{M}} + \frac{2D_0}{\varphi_0} \nabla \mu_{\mathcal{M}} \nabla \varphi_0 + \tau_{\mathcal{M}}^{-1} \left(\bar{V}_x(D_\theta) - \mu_{\mathcal{M}} \right) + 2\tilde{\lambda}_E \sigma_{\mathcal{M}}^2 (V_T - \mu_{\mathcal{M}}) \\ &\quad + D_M \frac{\partial^2}{\partial D_\theta^2} \mu_{\mathcal{M}} + \frac{2D_M}{\varphi_0} \left(\frac{\partial}{\partial D_\theta} \mu_{\mathcal{M}} \right) \left(\frac{\partial}{\partial D_\theta} \varphi_0 \right). \end{aligned} \quad (\text{S13})$$

Here, we have introduced the renormalized learning rate, $\tilde{\lambda}_E = 2\lambda_E \alpha_T$. Applying the same timescale separation as introduced above, the space-dependence of $\mu_{\mathcal{M}}(D_\theta, \mathbf{x}, t)$ can be neglected and we can therefore derive the relation,

$$\frac{\partial \mu_{\mathcal{M}}(D_\theta, t)}{\partial t} = \tau_{\mathcal{M}}^{-1} \left(\bar{V}_x(D_\theta) - \mu_{\mathcal{M}}(D_\theta, t) \right), \quad (\text{S14})$$

which corresponds to Eq. (23) of the main manuscript. Within this approximation $\sigma_{\mathcal{M}}^2$ becomes independent of the position and the policy, $\sigma_{\mathcal{M}}^2(D_\theta, \mathbf{x}, t) = \sigma_{\mathcal{M}}^2(t)$ and thus drops out in the equation for φ_0 . Our goal is to expand φ_0 in moments of D_θ and thus derive relations for the policy dynamics described by its mean and variance. We therefore expand $\mu_{\mathcal{M}}(\mathbf{x}, D_\theta, t)$ around a predefined policy $D_{\theta, E} = \mathcal{P}_E$,

$$\frac{\partial \mu_{\mathcal{M}}^{(n)}(t)}{\partial t} = \tau_{\mathcal{M}}^{-1} \left(\bar{V}_x^{(n)} - \mu_{\mathcal{M}}^{(n)}(t) \right), \quad (\text{S15})$$

with the n -th derivative $F^{(n)} = \left. \frac{\partial^n F(D_\theta)}{\partial D_\theta^n} \right|_{D_\theta = D_{\theta, E}}$. This allows us to write

$$\mu_{\mathcal{M}}(D_\theta, t) = \tilde{\mu}_{\mathcal{M}}^{(0)}(t) + \mu_{\mathcal{M}}^{(1)}(t) D_\theta + \mathcal{O}((D_\theta - D_{\theta, E})^2), \quad (\text{S16})$$

with $\tilde{\mu}_{\mathcal{M}}^{(0)}(t) = \mu_{\mathcal{M}}^{(0)}(t) - \mu_{\mathcal{M}}^{(1)}(t) D_{\theta, E}$. Consistent with the main manuscript we also define $V_E = \bar{V}_x(D_{\theta, E})$ and $V'_E = \partial \bar{V}_x(D_\theta) / \partial D_\theta |_{D_\theta = D_{\theta, E}}$. Finally, we assume that $\varphi_0(D_\theta, \mathbf{x}, t)$ is Gaussian and expand it in terms of its moments, $\rho(\mathbf{x}, t) = \int dD_\theta \varphi_0(D_\theta, \mathbf{x}, t)$, the average policy $\mu(\mathbf{x}, t) = \rho(\mathbf{x}, t)^{-1} \int dD_\theta D_\theta \varphi_0(D_\theta, \mathbf{x}, t)$, and the diversity $\sigma^2(\mathbf{x}, t) = \rho(\mathbf{x}, t)^{-1} \int dD_\theta (D_\theta - \mu(\mathbf{x}, t))^2 \varphi_0(D_\theta, \mathbf{x}, t)$. This yields the analytical hydrodynamic equations,

$$\frac{\partial \rho(\mathbf{x}, t)}{\partial t} = -\nabla (V_E + V'_E \mu(\mathbf{x}, t) - D_0 \nabla) \rho(\mathbf{x}, t) \quad (\text{S17})$$

$$\begin{aligned} \frac{\partial \mu(\mathbf{x}, t)}{\partial t} &= -(V_E + V'_E \mu(\mathbf{x}, t)) \nabla \mu(\mathbf{x}, t) - V'_E \nabla \sigma^2(\mathbf{x}, t) - V'_E \rho(\mathbf{x}, t)^{-1} \sigma^2(\mathbf{x}, t) \nabla \rho(\mathbf{x}, t) + D_0 \Delta \mu(\mathbf{x}, t) \\ &\quad + 2D_0 \rho(\mathbf{x}, t)^{-1} \nabla \mu(\mathbf{x}, t) \nabla \rho(\mathbf{x}, t) - 2\tilde{\lambda}_E \mu_{\mathcal{M}}^{(1)}(t) \sigma^2(\mathbf{x}, t) \rho(\mathbf{x}, t) \left(\tilde{\mu}_{\mathcal{M}}^{(0)}(t) - V_T + \mu_{\mathcal{M}}^{(1)}(t) \mu(\mathbf{x}, t) \right) \end{aligned} \quad (\text{S18})$$

$$\begin{aligned} \frac{\partial \sigma^2(\mathbf{x}, t)}{\partial t} &= -(V_E + V'_E \mu(\mathbf{x}, t)) \nabla \sigma^2(\mathbf{x}, t) - 2V'_E \sigma^2(\mathbf{x}, t) \nabla \mu(\mathbf{x}, t) + D_0 \Delta \sigma^2(\mathbf{x}, t) \\ &\quad + 2D_0 \rho(\mathbf{x}, t)^{-1} \nabla \sigma^2(\mathbf{x}, t) \nabla \rho(\mathbf{x}, t) + 2D_0 (\nabla \mu(\mathbf{x}, t))^2 + 2D_M - 2\tilde{\lambda}_E \rho(\mathbf{x}, t) \mu_{\mathcal{M}}^{(1)}(\mathbf{x}, t)^2 \sigma^2(\mathbf{x}, t)^2. \end{aligned} \quad (\text{S19})$$

These equations combine the convection and diffusion induced transport of policies and diversity, as well as the learning of new policies in the terms including $\tilde{\lambda}_E$. Connecting the equations to the kinetic theory results shown in the main manuscript, Eqs. (9) and (10), we therefore find,

$$F_1(\mu, \sigma^2; \mu_{\mathcal{M}}^{(n)}) = -2\tilde{\lambda}_E \mu_{\mathcal{M}}^{(1)} \left(\tilde{\mu}_{\mathcal{M}}^{(0)} - V_T + \mu_{\mathcal{M}}^{(1)} \mu \right) \quad (\text{S20})$$

$$F_2(\mu, \sigma^2; \mu_{\mathcal{M}}^{(n)}) = 2\tilde{\lambda}_E \mu_{\mathcal{M}}^{(1)2}. \quad (\text{S21})$$

C. Analytical solutions for fixed targets

In the following we assume that both the target velocity V_T and the initial conditions are independent of position \mathbf{x} . Furthermore, we assume timescale separation between $\tau_{\mathcal{M}}$ and λ_E and thus replace $\mu_{\mathcal{M}}^{(n)}(t)$ by their steady-state

values. We thus find,

$$\frac{d\mu(t)}{dt} = -2\tilde{\lambda}_E V_E'^2 \sigma^2(t) \rho(\mu(t) - D_{\theta,T}) \quad (\text{S22})$$

$$\frac{d\sigma^2(t)}{dt} = 2D_M - 2\tilde{\lambda}_E \rho V_E'^2 \sigma^2(t)^2. \quad (\text{S23})$$

where $D_{\theta,T} = D_{\theta,E} + (V_T - V_E)/V_E'$ is an approximation of the target policy which maximizes the reward. In particular, if $V_E \rightarrow V_T$ the relation becomes exact. Thus it is important to choose an appropriate $D_{\theta,E}$. From these dynamical equations we can directly derive Eqs. (12) and (13) as stated in the main manuscript.

D. Analytical solution for space-dependent targets

We are also interested in the steady-state solution in the presence of a space-dependent target $V_T(x) = V_T^s + V_T^\Delta \sin(2\pi x/L)$. We assume that D_0/L^2 is significantly smaller than v_0/L and thus convective transport dominates. Furthermore, we expect that the spatial dependency of $\rho(\mathbf{x}, t)$ and $\sigma^2(\mathbf{x}, t)$ are significantly smaller than the one of $\mu(\mathbf{x}, t)$. Finally, we assume that the convection velocity in the steady-state $V_0 + V_E' \mu(\mathbf{x}, t) \approx V_T^s$, thus neglecting higher-order terms. Under these approximations we can derive that $\sigma^2(\mathbf{x}, t) = \sqrt{\frac{2D_M}{\lambda}}$ with $\lambda_0 = 2\tilde{\lambda}_E \rho V_E'^2$ and thus find the partial differential equation,

$$0 = -V_T^s \nabla \mu(x) - \sqrt{2D_M \lambda} (\mu(x) - D_{\theta,T}(x)), \quad (\text{S24})$$

where $D_{\theta,T}(x) = D_{\theta,E} + (V_T(x) - V_0)/V_E'$. This equation corresponds to Eq. (14) in the main manuscript.

To solve this equation we are using ansatz, $\mu(x) = \mu_T^s + \mu_T^\Delta \sin(2\pi x/L + \phi)$ which yields explicit relations for μ_T^s , μ_T^Δ and ϕ . Finally, we identify the average velocity $\langle V_x(x) \rangle = V(D_{\theta,E}) + V_E'(\mu(x) - D_{\theta,E})$, which yields the relations stated in the main manuscript.

E. Numerical details

To enable reproducibility we list in the following all the parameters used in the agent-based simulations, which are described in the main manuscript,

- $\tau_B = 0.004$
- $\sigma_B = 0.1$
- $\tau_M = 1.0$
- $\lambda_E^{-1} = 100$
- $v_0 = 1, D_0 = 0.0001$
- $\alpha_T = 10$, corresponding to a very steep activation function.
- $N = 10000$
- $L_x = L_y = 10 \rightarrow \rho = 100$. Only for Fig. 3 we have set $L_x = 100$ keeping the density constant, i.e. choosing $N = 10^5$.
- $\Delta t = 0.002$ which is small enough to capture the smallest timescales.
- $r_c = \frac{1}{\sqrt{\pi}}$, to ensure that each particle has approximately ρ particles in its communication neighborhood. This ensures consistency with the kinetic theory.
- $\mu(t=0) = 100, \sigma^2(t=0) = 400$.

Goal: Maximize $\langle I \rangle$ by adapting robot speed

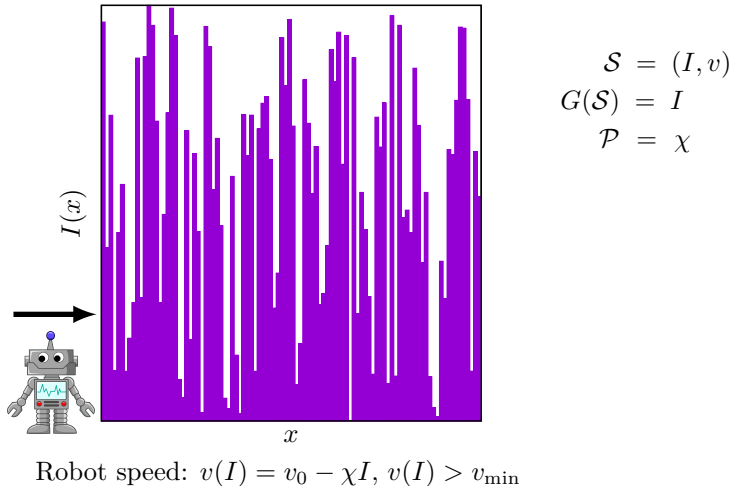


FIG. S2. Illustration of MODEL2, featuring non-interacting robots which attempt to maximize the light-intensity $\langle I \rangle$ to which they are exposed by learning the optimal parameter χ controlling their local movement speed.

II. DERIVATIONS FOR MODEL2: ROBOTS

The second model represents a robot moving in a landscape of space-dependent external light intensity. The model is one-dimensional and we assume that space is separated into N_{bin} equally-sized bins i of size ΔL . Each bin has light intensity I_i , which are uncorrelated in space and equally distributed in $I_i \in [0, I_{\max}]$ thus forming the intensity field $I(x)$, which can be measured by the robot. The speed of the robot is then defined as $v(I) = v_0 - \chi I$ and capped at $v_{\min} > 0$ (thus the robot always moves forward). The parameter χ thus defines the sensitivity with which the robot reacts to the external light. The state of the robot is therefore $\mathcal{S} = (I, v)$. We apply periodic boundary conditions, but generally assume L to be large compared to ΔL . We assume that we have N robots in the world, but robots do not interact with each other (apart from the learning). The goal of each robot is to adjust the policy $\mathcal{P} = \chi$ such that it maximizes $\bar{I}(\chi) = \langle I(x) \rangle_{\chi}$, i.e., the average light intensity seen by a robot with sensitivity χ .

A. Solving the microscopic physical model

The probability for each robot to be in bin i with intensity I_i is,

$$p(I) \propto v(I)^{-1} = \begin{cases} (v_0 - \chi I)^{-1}, & \text{for } I < I^* \\ v_{\min}^{-1}, & \text{for } I \geq I^* \end{cases} \quad (\text{S25})$$

with $I^* = \frac{v_0 - v_{\min}}{\chi}$. Assuming that the physical time scale $\Delta L/v_0$ is much smaller than any other time scale in the system, i.e., that each robot sees many different I_i on the memory time scale $\tau_{\mathcal{M}}$, we can then calculate the expected average light-intensity seen by the robot with policy χ ,

$$\bar{I}(\chi) = \frac{\int_0^{I_{\max}} dI I p(I)}{\int_0^{I_{\max}} dI p(I)}. \quad (\text{S26})$$

The integral can be separated into two parts going from $[0, I^*]$ and $[I^*, I_{\max}]$ and then solved easily. The final result is,

$$\bar{I}(\chi) = \begin{cases} \left[\frac{1}{2v_{\min}} (I_{\max}^2 - I^{*2}) - \frac{I^*}{\chi} + \frac{v_0}{\chi^2} \ln(v_0/v_{\min}) \right] \left[\frac{I_{\max} - I^*}{v_{\min}} + \frac{1}{\chi} \ln\left(\frac{v_0}{v_{\min}}\right) \right]^{-1}, & \text{for } \chi > \frac{v_0 - v_{\min}}{I_{\max}} \\ \frac{v_0}{\chi} - \frac{I_{\max}}{\ln(v_0/(v_0 - \chi I_{\max}))}, & \text{otherwise} \end{cases} \quad (\text{S27})$$

In MODEL2 we choose $G(\mathcal{S}) = I$, thus $\bar{I}(\chi)$ directly corresponds to the term $\bar{G}(\mathcal{P})$ introduced in the main manuscript. Different from MODEL1 we then choose as reward function $\mathcal{R}(\mathcal{M}) = \mathcal{M}$ since we aim at maximizing the collected light intensity. We thus find for Eqs. (22) and (23) in the main manuscript (dropping any space dependence on longer

time scales and assuming time scale separation),

$$\frac{\partial \varphi_0(\chi, t)}{\partial t} = \tilde{\lambda}_E \varphi_0 \int d\chi' \varphi_0(\chi', t) \mu_{\mathcal{M}}(\chi', t) - \tilde{\lambda}_E \varphi_0 \rho(t) \mu_{\mathcal{M}} + D_M \frac{\partial^2}{\partial \chi^2} \varphi_0 \quad (\text{S28})$$

$$\frac{\partial \mu_{\mathcal{M}}(\chi, t)}{\partial t} = \tau_{\mathcal{M}}^{-1} \left(\bar{I}(\chi) - \mu_{\mathcal{M}} \right). \quad (\text{S29})$$

To capture the details of $\bar{I}(\chi)$ we expand it to fourth order. As before, we expand around a predefined policy χ_E ,

$$\frac{\partial \mu_{\mathcal{M}}^{(n)}(t)}{\partial t} = \tau_{\mathcal{M}}^{-1} \left(\bar{I}^{(n)} - \mu_{\mathcal{M}}^{(n)}(t) \right), \quad (\text{S30})$$

with the n -th derivative $F^{(n)} = \left. \frac{\partial^n F(\chi)}{\partial \chi^n} \right|_{\chi=\chi_E}$. This allows us to write

$$\mu_{\mathcal{M}}(\chi, t) = \tilde{\mu}_{\mathcal{M}}^{(0)}(t) + \tilde{\mu}_{\mathcal{M}}^{(1)}(t)\chi - \tilde{\mu}_{\mathcal{M}}^{(2)}(t)\chi^2 + \tilde{\mu}_{\mathcal{M}}^{(3)}(t)\chi^3 - \tilde{\mu}_{\mathcal{M}}^{(4)}(t)\chi^4, \quad \text{with} \quad (\text{S31})$$

$$\tilde{\mu}_{\mathcal{M}}^{(0)}(t) = \mu_{\mathcal{M}}^{(0)}(t) - \mu_{\mathcal{M}}^{(1)}(t)\chi_E + \frac{1}{2}\mu_{\mathcal{M}}^{(2)}(t)\chi_E^2 - \frac{1}{6}\mu_{\mathcal{M}}^{(3)}(t)\chi_E^3 + \frac{1}{24}\mu_{\mathcal{M}}^{(4)}(t)\chi_E^4, \quad (\text{S32})$$

$$\tilde{\mu}_{\mathcal{M}}^{(1)}(t) = \mu_{\mathcal{M}}^{(1)}(t) - \mu_{\mathcal{M}}^{(2)}(t)\chi_E + \frac{1}{2}\mu_{\mathcal{M}}^{(3)}(t)\chi_E^2 - \frac{1}{6}\mu_{\mathcal{M}}^{(4)}(t)\chi_E^3 \quad (\text{S33})$$

$$\tilde{\mu}_{\mathcal{M}}^{(2)}(t) = -\frac{1}{2}\mu_{\mathcal{M}}^{(2)}(t) + \frac{1}{2}\mu_{\mathcal{M}}^{(3)}(t)\chi_E - \frac{1}{4}\mu_{\mathcal{M}}^{(4)}(t)\chi_E^2, \quad (\text{S34})$$

$$\tilde{\mu}_{\mathcal{M}}^{(3)}(t) = \frac{1}{6}\mu_{\mathcal{M}}^{(3)}(t) - \frac{1}{6}\mu_{\mathcal{M}}^{(4)}(t)\chi_E \quad (\text{S35})$$

$$\tilde{\mu}_{\mathcal{M}}^{(4)}(t) = -\frac{1}{24}\mu_{\mathcal{M}}^{(4)}(t). \quad (\text{S36})$$

Inserting this expansion into Eq. (S28) and using the same moments, average policy μ and diversity σ^2 , as for MODEL1, we finally find,

$$\frac{\partial \mu(t)}{\partial t} = -\tilde{\lambda}_E \rho \sigma^2(t) \left(\tilde{\mu}_{\mathcal{M}}^{(1)}(t) - 2\tilde{\mu}_{\mathcal{M}}^{(2)}(t)\mu(t) \right) \quad (\text{S37})$$

$$\frac{\partial \sigma^2(t)}{\partial t} = 2D_M - 2\tilde{\lambda}_E \rho \sigma^2(t)^2 \left(\tilde{\mu}_{\mathcal{M}}^{(2)}(t) - 3\tilde{\mu}_{\mathcal{M}}^{(3)}(t)\mu(t) + 6\tilde{\mu}_{\mathcal{M}}^{(4)}(t)(\mu(t)^2 + \sigma^2(t)) \right). \quad (\text{S38})$$

These equations have been used for the numerical results shown in Fig. 4 in the main manuscript.

B. Numerical details

The following parameters were used in the agent-based simulations,

- $\Delta L = 10^{-3}$
- $\tau_{\mathcal{M}} = 1.0$
- $\lambda_E^{-1} = 100$
- $v_0 = 1, v_{\min} = 0.01$
- $D_0 = 0$
- $\alpha_T = 10$, corresponding to a very steep activation function.
- $N = 10000$
- $L = 100 \rightarrow \rho = 100$.
- $\Delta t = 0.0001$ which is small enough to capture the smallest timescales.
- $r_c = 0.5$, to ensure that each particle has approximately ρ particles in its communication neighborhood. This ensures consistency with the kinetic theory.
- $\mu(t=0) = 1.25, \sigma^2(t=0) = 0.0225$.

III. MULTI-DIMENSIONAL KINETIC THEORY

We have emphasized in the main manuscript that the state \mathcal{S} , the memory \mathcal{M} and the policy \mathcal{P} could be multi-dimensional. Here, we show that one can similarly derive hydrodynamic equation in such a situation. (Ignoring space to keep the notation more compact.)

The multi-dimensionality starts to play a role once we introduce the moments in the memory, including the density, $\varphi_0(\mathcal{P}, t) = \int d\mathcal{M} f_0(\mathcal{M}, \mathcal{P}, t)$, the average memory, $\mu_{\mathcal{M},i}(\mathcal{P}, t) = \varphi_0^{-1} \int d\mathcal{M} \mathcal{M}_i f_0(\mathcal{M}, \mathcal{P}, t)$ and the memory covariance matrix, $\sigma_{\mathcal{M},ij}^2(\mathcal{P}, t) = \varphi_0^{-1} \int d\mathcal{M} (\mathcal{M}_i - \mu_{\mathcal{M},i}(\mathcal{P}, t)) (\mathcal{M}_j - \mu_{\mathcal{M},j}(\mathcal{P}, t)) f_0(\mathcal{M}, \mathcal{P}, t)$. As in MODEL1 we assume that $\mathcal{R}(\mathcal{M}) = 1 - \sum_i (\mathcal{M}_i - T_i)^2$, i.e., we want that each entry in the memory approaches a certain target T_i . Assuming the time scale hierarchy, $\tau_G \ll \tau_{\mathcal{M}} \ll \tau_E$, we then find for the policy dynamics,

$$\begin{aligned} \frac{\partial \varphi_0(\mathcal{P}, t)}{\partial t} &= \tilde{\lambda}_E \varphi_0 \int d\mathcal{P}' \varphi_0(\mathcal{P}', t) \sum_i \left(\sigma_{\mathcal{M},ii}^2(\mathcal{P}', t) + \mu_{\mathcal{M},i}(\mathcal{P}', t)^2 - 2T_i \mu_{\mathcal{M},i}(\mathcal{P}', t) \right) \\ &\quad + \tilde{\lambda}_E \varphi_0 \rho(t) \sum_i \left(2T_i \mu_{\mathcal{M},i} - \mu_{\mathcal{M},i}^2 - \sigma_{\mathcal{M},ii}^2 \right) + D_M \frac{\partial^2}{\partial \mathcal{P}^2} \varphi_0 \end{aligned} \quad (\text{S39})$$

$$\frac{\partial \mu_{\mathcal{M},i}(\mathcal{P}, t)}{\partial t} = \tau_{\mathcal{M}}^{-1} \left(\bar{G}_i(\mathcal{P}) - \mu_{\mathcal{M},i} \right). \quad (\text{S40})$$

As in the main manuscript, we denote as $\bar{G}_i(\mathcal{P}) = \langle G_i(\mathcal{S}) \rangle_{\mathcal{P}}$ the policy-dependent ensemble average of the information $G_i(\mathcal{S})$. We can then expand the memory $\mu_{\mathcal{M},i}(\mathcal{P}, t)$ around a predefined policy $D_{\theta,E} = \mathcal{P}_E$, by introducing the quantities $\mu_{\mathcal{M},i}^{(0)} = \mu_{\mathcal{M},i}(\mathcal{P}_E)$, $\mu_{\mathcal{M},ij}^{(1)}(t) = \left. \frac{\partial \mu_{\mathcal{M},i}(\mathcal{P})}{\partial \mathcal{P}_j} \right|_{\mathcal{P}=\mathcal{P}_E}$, $\bar{G}_{E,i} = \bar{G}_i(\mathcal{P}_E)$ and $\bar{G}'_{E,ij} = \left. \frac{\partial \bar{G}_i(\mathcal{P})}{\partial \mathcal{P}_j} \right|_{\mathcal{P}=\mathcal{P}_E}$. We thus find,

$$\frac{\partial \mu_{\mathcal{M},i}^{(0)}(t)}{\partial t} = \tau_{\mathcal{M}}^{-1} \left(\bar{G}_{E,i} - \mu_{\mathcal{M},i}^{(0)}(t) \right), \quad (\text{S41})$$

$$\frac{\partial \mu_{\mathcal{M},ij}^{(1)}(t)}{\partial t} = \tau_{\mathcal{M}}^{-1} \left(\bar{G}'_{E,ij} - \mu_{\mathcal{M},ij}^{(1)}(t) \right). \quad (\text{S42})$$

This allows us to expand the memory, $\mu_{\mathcal{M},i}(\mathcal{P}, t) = \tilde{\mu}_{\mathcal{M},i}^{(0)}(t) + \mu_{\mathcal{M},ij}^{(1)}(t) \mathcal{P}_j$, with $\tilde{\mu}_{\mathcal{M},i}^{(0)}(t) = \mu_{\mathcal{M},i}^{(0)}(t) - \mu_{\mathcal{M},ij}^{(1)}(t) D_{\theta,E,j}$, using Einstein summation convention.

As described before after Eq. (S14), we find that $\sigma_{\mathcal{M}}^2$ is independent of \mathcal{P} when assuming timescale separation and thus can be canceled out. Finally, we assume that $\varphi_0(\mathcal{P}, t)$ is Gaussian and expand it in terms of its moments, the average policy $\mu_i(t) = \rho(t)^{-1} \int d\mathcal{P} \mathcal{P}_i \varphi_0(\mathcal{P}, t)$, and the covariance $\sigma_{ij}^2(t) = \rho(t)^{-1} \int d\mathcal{P} (\mathcal{P}_i - \mu_i(t)) (\mathcal{P}_j - \mu_j(t)) \varphi_0(\mathcal{P}, t)$. We also identify higher moments for multi-dimensional Gaussians

$$\int d\mathcal{P} (\mathcal{P}_i - \mu_i(t)) (\mathcal{P}_j - \mu_j(t)) (\mathcal{P}_k - \mu_k(t)) \varphi_0(\mathcal{P}, t) = 0 \quad (\text{S43})$$

$$\Rightarrow \rho(t)^{-1} \int d\mathcal{P} \mathcal{P}_i \mathcal{P}_j \mathcal{P}_k \varphi_0(\mathcal{P}, t) = \mu_i(t) \mu_j(t) \mu_k(t) + \mu_i(t) \sigma_{jk}^2(t) + \mu_j(t) \sigma_{ik}^2(t) + \mu_k(t) \sigma_{ij}^2(t) \quad (\text{S44})$$

$$\int d\mathcal{P} (\mathcal{P}_i - \mu_i(t)) (\mathcal{P}_j - \mu_j(t)) (\mathcal{P}_k - \mu_k(t)) (\mathcal{P}_l - \mu_l(t)) \varphi_0(\mathcal{P}, t) = \sigma_{ij}^2(t) \sigma_{kl}^2(t) + \sigma_{ik}^2(t) \sigma_{jl}^2(t) + \sigma_{il}^2(t) \sigma_{kj}^2(t) \quad (\text{S45})$$

$$\begin{aligned} \Rightarrow \rho(t)^{-1} \int d\mathcal{P} \mathcal{P}_i \mathcal{P}_j \mathcal{P}_k \mathcal{P}_l \varphi_0(\mathcal{P}, t) &= \mu_i(t) \mu_j(t) \mu_k(t) \mu_l(t) + \sigma_{ij}^2(t) \sigma_{kl}^2(t) + \sigma_{ik}^2(t) \sigma_{jl}^2(t) + \sigma_{il}^2(t) \sigma_{kj}^2(t) + \mu_i(t) \mu_j(t) \sigma_{kl}^2(t) \\ &\quad + \mu_i(t) \mu_k(t) \sigma_{jl}^2(t) + \mu_i(t) \mu_l(t) \sigma_{jk}^2(t) + \mu_j(t) \mu_k(t) \sigma_{il}^2(t) + \mu_j(t) \mu_l(t) \sigma_{ik}^2(t) + \mu_k(t) \mu_l(t) \sigma_{ij}^2(t). \end{aligned} \quad (\text{S46})$$

After some calculations we find,

$$\frac{\partial \mu_l(t)}{\partial t} = -2\tilde{\lambda}_E \rho \sum_i \mu_{\mathcal{M},ij}^{(1)} \sigma_{jl}^2(t) \left[\mu_{\mathcal{M},ik}^{(1)} \mu_k(t) - T_i + \tilde{\mu}_{\mathcal{M},i}^{(0)} \right] \quad (\text{S47})$$

$$\frac{\partial \sigma_{ln}^2(t)}{\partial t} = 2D_M \delta_{ln} - 2\tilde{\lambda}_E \rho \sum_i \mu_{\mathcal{M},ij}^{(1)} \mu_{\mathcal{M},ik}^{(1)} \sigma_{ij}^2 \sigma_{nk}^2 \quad (\text{S48})$$

While these equations are slightly more complex than the one-dimensional Eqs. (S18) and (S19), they still share very similar characteristics. For example, if the covariance for dimension l of the \mathcal{P}_l is zero, i.e., $\sigma_{kl}^2 = 0 \forall k$, we find immediately that $\partial \mu_l(t) / \partial t = 0$ as expected from Fisher's first theorem of natural selection [S4].

SUPPLEMENTARY REFERENCES

- [S1] M. Brun-Cosme-Bruny, E. Bertin, B. Coasne, P. Peyla, and S. Rafai, Effective diffusivity of microswimmers in a crowded environment, *The Journal of Chemical Physics* **150**, 104901 (2019), https://pubs.aip.org/aip/jcp/article-pdf/doi/10.1063/1.5081507/13951776/104901_1_online.pdf.
- [S2] M. Brun-Cosme-Bruny, A. Förtsch, W. Zimmermann, E. Bertin, P. Peyla, and S. Rafai, Deflection of phototactic microswimmers through obstacle arrays, *Phys. Rev. Fluids* **5**, 093302 (2020).
- [S3] A. Peshkov, E. Bertin, F. Ginelli, and H. Chaté, Boltzmann-ginzburg-landau approach for continuous descriptions of generic viscek-like models, *The European Physical Journal Special Topics* **223**, 1315 (2014).
- [S4] W. Ewens, An interpretation and proof of the fundamental theorem of natural selection, *Theoretical Population Biology* **36**, 167 (1989).